



Passivity and passivity breakdown of 304 stainless steel in alkaline sodium sulphate solutions

S.S. El-Egamy and W.A. Badaway*

Faculty of Science, Department of Chemistry, Cairo University, Giza, Egypt

(*author for correspondence, wbadaway@main-sec.cairo.eun.eg)

Received 31 March 2004; accepted in revised form 6 July 2004

Key words: corrosion, corrosion inhibition, EIS, passivation, pitting, stainless steel

Abstract

The passivity and passivity breakdown of 304 stainless steel were investigated in 0.25 M Na₂SO₄ solutions of pH 10. The effect of applied potential and the presence of Cl⁻ ions in the electrolyte were also studied. Different electrochemical methods such as open circuit potential measurements, polarization techniques and electrochemical impedance spectroscopy (EIS) were used. The results showed that the steel electrode passivates under open circuit conditions and also under potentiostatic control. The rate of passive film thickening under open circuit conditions follows a simple logarithmic law. Addition of Cl⁻ ion shifts the polarization curves in the active direction and above a critical chloride concentration, [Cl⁻] ≥ 0.15 M, pitting corrosion occurs and the pitting potential, E_{pit} , decreases linearly with the logarithm of [Cl⁻]. The addition of sulphate ions to the chloride-containing solutions was found to inhibit the pitting process, and at [SO₄²⁻] ≥ 0.25 M, a complete immunity to pitting corrosion was recorded. The impedance measurements provided support for film thickening and film breakdown reactions. An equivalent circuit model which consists of a pure resistor, R_{Ω} , in series with a parallel combination of a pure resistor, R_p , and a constant phase element, Q , was proposed to describe the electrode/electrolyte interface. The passive film thickness was found to increase with applied potential up to a critical value of 0.3 V. At higher voltages, breakdown of the passive film occurred.

1. Introduction

The nature and composition of passive films formed on stainless steels, and especially their protective nature, are dependent on the formation conditions, e.g. the passivation potential, ageing, electrolyte composition and temperature. Stable passive films formed on alloys with compositions close to the 304 and 316 stainless steels are heterogeneous. These films are described by a bilayer structure, composed essentially of a chromium hydroxide, Cr(OH)₃, outer layer and a mixed inner layer of chromium and iron oxides, enriched in chromium [1, 2]. This structure is similar to that produced on passivated ferritic iron-chromium alloys [3, 4].

It is well known that passive films formed on metals in the presence of chloride ions are less stable due to local damage and pitting corrosion. The penetration effect and pitting properties of Cl⁻ depend on the experimental conditions [4–6]. However, the presence of non-aggressive anions like sulphate SO₄²⁻, chromate CrO₄²⁻, bicarbonate HCO₃⁻, and phosphate PO₄³⁻, in aqueous solutions plays an important role in the passivation process [7–9]. They tend to reduce the susceptibility of stainless steel to pitting in chloride solutions.

The passivity of stainless steel was attributed to the formation of chromium oxide barrier layer [10]. The incorporation of anions such as CrO₄²⁻ or SO₄²⁻ leads to further growth of the barrier layer as well as impeding the ingress of OH⁻ and Cl⁻. The early stages of pitting on passivated 304 stainless steel in 0.25 M NaCl solution at low potential have been studied by AC impedance [11]. The authors found that the reaction is charge transfer controlled at potentials below –200 mV (sce). At higher potentials, charge transfer and diffusion processes occurred at the electrode surface. The charge transfer resistance, R_{ct} , was found to decrease with increasing temperature and increasing Cl⁻ concentration [12]. There exists a minimum chloride ion concentration above which pit propagation exists.

Although sulphate ions are well known to facilitate film growth [13], and act as pitting inhibitor [7], the presence of these ions together with chloride ions leads to stronger attack and produces larger pits compared to those obtained in sulphate free chloride solutions [14–16].

This phenomenon is important for the manufacture of NaCl and Na₂SO₄ from concentrated marine (brine) solution. Steel pipes are used in the sulphate production unit (EMISAL) from Quaroun lake, Egypt, and

experience degradation due to continuous pitting. This paper describes an investigation of the pitting corrosion and passivation properties of steel samples in alkaline sulphate solutions. The solution pH was selected to simulate that of the sulphate production unit. In these investigations conventional electrochemical techniques and electrochemical impedance spectroscopy (EIS) were used under open-circuit and polarization conditions. The optimum sulphate/chloride ratio to achieve minimum corrosion rate was suggested.

2. Experimental details

The working electrodes were made from stainless steel samples used in the heat exchanger tubes used in the production of sodium sulphate. The mass spectroscopic analysis of this material is presented in Table 1. The test electrodes with exposed surface area of 0.124 cm² were prepared and pretreated as described previously [5]. The electrolytic cell was an all glass double jacket three-electrode cell with a spiral platinum counter electrode and a saturated calomel reference electrode. The test solutions were prepared from analytical grade reagents and triply distilled water. The pH was adjusted to pH=10 by sodium hydroxide stock solution. All measurements were carried out in naturally aerated solutions at a constant room temperature of 25 °C ± 0.1. All potentials were measured against and referred to the saturated calomel electrode using a high impedance digital valve voltmeter.

Polarization experiments were performed using a potentiostat/galvanostat interfaced to a personal computer. Potentiodynamic polarization runs were conducted at a scan rate of 1 mV s⁻¹ and in the potential range -0.4 to +1.5 V or to the beginning of stable pitting. Potentiostatic experiments were carried out by applying constant potentials in the range -0.4 to 1.3 V at 200 mV increments. The current transient at each applied potential was recorded for a period of 30 min, where a steady minimum current was reached. Electrochemical impedance spectroscopy, EIS, investigations both under open circuit condition or potentiostatic polarization were carried out using the IM5d-AMOS system (Zahner Elektrik GmbH & Co., Kronach, Germany). The amplitude of the superimposed ac signal was 10 mV peak to peak. The method involves direct measurement of the impedance, *Z* and the phase shift, *θ*, of the electrochemical system in the frequency domain from 0.1 to 10⁵ Hz. Details of experimental procedures are as described elsewhere [5, 6].

3. Results and discussion

3.1. Open circuit measurements

The corrosion potential of the steel electrode was recorded with time over a period of 4 h in 0.25 M Na₂SO₄ solution of pH 10. The cell impedance, *Z*, and the phase shift, *θ*, were recorded at different time intervals. The open circuit potential gets more positive with time indicating passivation of the steel electrode in the alkaline sulphate solution. The variation of the steel electrode potential, *E*, with time is shown in Figure 1. The potential increases with time following a simple logarithmic law [6],

$$E = \alpha + \beta \log(t + t_0) \quad (1)$$

where *α* is a constant and *β* represents the rate coefficient of passive film growth. The *E* versus log *t* relation consists of two linear segments with different slopes *β*₁ and *β*₂ (cf. Figure 1). The first segment with the smaller slope *β*₁ is related to anion adsorption. At longer time of electrode immersion (*t* > 6 min) film thickening dominates with a larger rate corresponding to *β*₂.

At open circuit potential, where the surface is not perturbed, sulphate adsorption is a relatively fast process and the steady state surface concentration is established within 5 min [17]. The mobility of anions in electrolyte, especially sulphate depends on the solution pH, i.e. increase in solution pH leads to a decrease in the mobility of ions, which shows a minimum at pH 10 [17]. At longer time of electrode immersion (*t* > 6 min), the surface is completely covered with anions which are incorporated within the passive film leading to further thickening. Thus a higher slope, *β*₂, of the second segment is recorded. These results are in agreement with the previous work, which showed that passive films

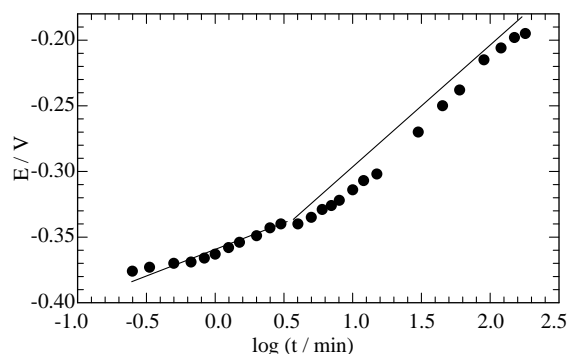


Fig. 1. Variation of the corrosion potential, *E*, with the logarithm of the time for type 304 stainless steel in 0.25 M Na₂SO₄ at pH 10.

Table 1. Mass spectrometric analysis of the steel sample

Element	C	Si	Mn	P	S	Cr	Ni	Ti
%	0.06	0.53	0.21	0.026	0.016	17.45	9.80	0.57

formed on iron in alkaline sulphate solutions are thicker than those formed in sulphate free alkaline solutions [13]. The corrosion and passivation of the steel involves competitive dissolution and film formation reactions. The net rate of film thickening is low in the first few minutes, where the dissolution process is dominant. After longer immersion time, the surface becomes covered by corrosion products and the rate of dissolution decreases. In this case film formation dominates and the surface becomes passive leading to a progressive increase in potential [18, 19]. The break in the E vs. $\log t$ relation can be attributed to the nature of the passive film. The passive film on steels consists mainly of a barrier inner layer of Cr_2O_3 and an outer layer of corrosion products that can incorporate ions from the solution leading to a change in the rate of film thickening with longer immersion time and the recorded increase of potential [6, 20, 21].

The results of open-circuit impedance measurements provide further evidence for film thickening in alkaline sulphate solutions. Figure 2 shows typical Bode diagrams recorded at different immersion times of the steel electrode in alkaline 0.25 M Na_2SO_4 . There is a general trend of increasing electrode impedance, Z , with time indicating film thickening and passivation of the surface. The Bode plots show typical capacitive like behaviour with one time constant. They also show phase angle maxima smaller than 90° ($\sim 72^\circ$), and absolute values of the impedance modulus slope lower than unity (~ 0.81). The phase angle deviation can be interpreted as a deviation of the double layer from ideal capacitance behaviour. Such behaviour is termed a frequency dispersion and considered to be due to local inhomogeneities in the dielectric material, porosity, mass transport and relaxation effects [22, 23]. An electric equivalent circuit model has been proposed to account for such frequency dispersion [24]. This model consists of a pure resistance, R_Ω , in series with a parallel combination of ideal resistance, R_p , and a constant

phase element, Q , (cf. Figure 2b). The constant phase element, Q , has been introduced as a substitute for capacitance to account for such frequency dispersion.

The total impedance of such systems can be represented by the following transfer functions [25]:

$$Z(\omega) = R_\Omega + \frac{R_p}{1 + (Q(j\omega)^\alpha)} \quad (2)$$

where $\omega = 2\pi f$ is the angular frequency, R_p the polarization (or passive film) resistance, $j = \sqrt{-1}$, Q the constant phase element and α is a fit parameter which is related to the surface roughness, where $0 \leq \alpha \leq 1$. It measures the deviation from the ideal capacitive behaviour. The impedance of the constant phase element is given by

$$Z_{\text{CPE}} = k^{-1}(j\omega)^{-\alpha} \quad (3)$$

The experimental results correspond to this function in a frequency range from 15 kHz to 1 Hz, and the constant phase element, Q , is given by R_p and K .

$$Q = R_p K \quad (4)$$

If the frequency dispersion is neglected i.e when $\alpha \rightarrow 1$, then K corresponds to the capacitance, C , [26] and that the reciprocal of the capacitance C^{-1} is directly proportional to the thickness of the passive film [27].

The experimental impedance data were analyzed using software provided with the impedance system, which enables data fitting in the required frequency range. For data fitting, Bode plots are recommended since all data are equally represented and the phase angle is a sensitive parameter to surface changes at the electrode/electrolyte interface [22]. The calculated equivalent circuit parameters for the steel electrode passivated under open circuit condition in sulphate solution are presented in Table 2. The average value of the parameter α is 0.81 and permits use of the capacitance without any correction to account for constant phase element [26]. Plots of both R_p and the reciprocal of the capacitance C^{-1} versus the logarithm of the time are presented in Figure 3. The linear relations of this figure can be represented by the following equations

$$R_p = \alpha' + \beta' \log(t + t_0) \quad (5)$$

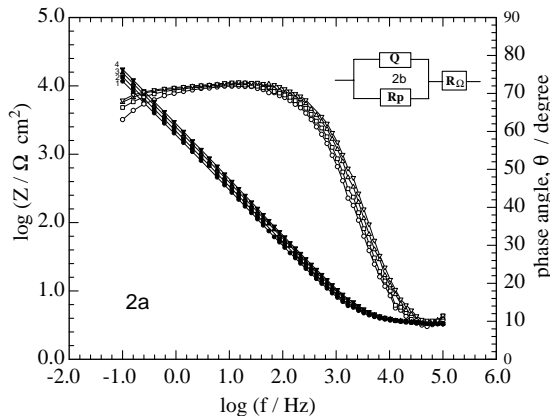


Fig. 2. (a) Bode plots for type 304 SS at different immersion times: (1) 15, (2) 30, (3) 60 and (4) 120 min. (b) Equivalent circuit model used to describe the steel electrode/electrolyte interface at different conditions; R_Ω = solution resistance, R_p = passive film resistance, Q = constant phase element.

Table 2. Equivalent circuit parameters for type 304 stainless steel at different immersion times in 0.25 M Na_2SO_4 solution of pH 10

Time /min	R_Ω / Ω cm ²	R_p /M Ω cm ²	C / μF cm ⁻²	α
15	25.58	0.53	22.18	0.81
30	25.75	0.87	19.93	0.81
60	25.51	1.31	17.67	0.81
90	25.59	1.38	16.49	0.82
120	25.37	1.58	15.77	0.81
150	15.32	1.62	15.34	0.81
180	25.30	1.74	15.15	0.81
240	25.30	1.63	14.65	0.81

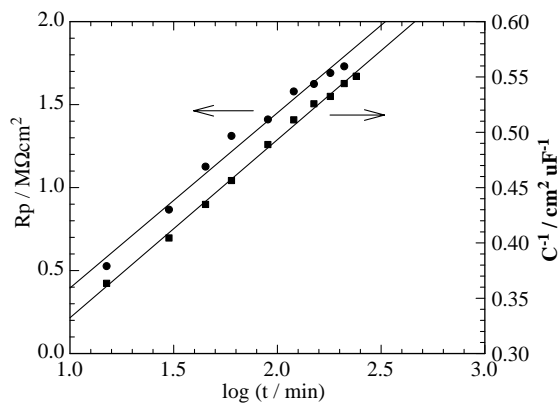


Fig. 3. Variation of R_p and C^{-1} with the logarithm of the immersion time for the steel electrode in 0.25 M Na_2SO_4 solution of pH 10.

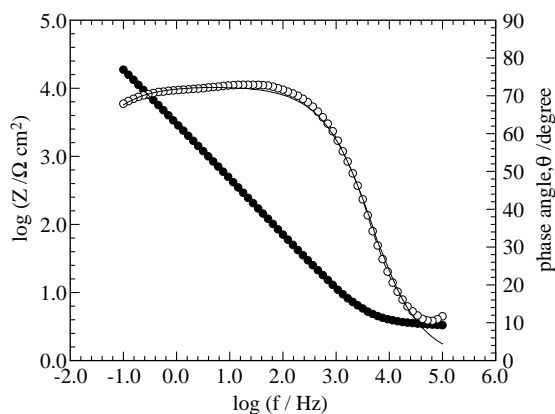


Fig. 4. (o) Experimental impedance data for type 304 SS electrode passivated at 0.3 V in 0.25 M Na_2SO_4 at pH 10 and (-) the theoretical one calculated according to the model presented in Figure 2b, with the values $R_\Omega=32.4 \Omega$, $R_p=4.380 \text{ M}\Omega \text{ cm}^2$, $C=6.702 \mu \text{ F cm}^{-2}$ and $\alpha=0.85$.

$$C^{-1} = \alpha' + \beta'' \log(t + t_0) \quad (6)$$

where β' and β'' are the rate coefficients of the film thickening analogous to the β value in Equation 1. The experimental impedance data for the steel electrode recorded after 120 min were fitted to the theoretical values calculated according the model shown in Figure 2b, and presented in Figure 4. The good fit of Figure 4 indicates the validity of the proposed model to fit the electrode/electrolyte interface of the investigated steel in the alkaline sulphate solution.

3.2. Potentiodynamic polarization results

3.2.1. Effect of chloride ion concentration

Figure 5a shows the potentiodynamic polarization curves recorded for the steel electrodes in chloride free and chloride containing sulphate solutions. In the absence of Cl^- , the steel electrode is passive over a wide potential range extending from -0.4 to 1.3 V (sce). At higher potentials a sharp increase in current due to

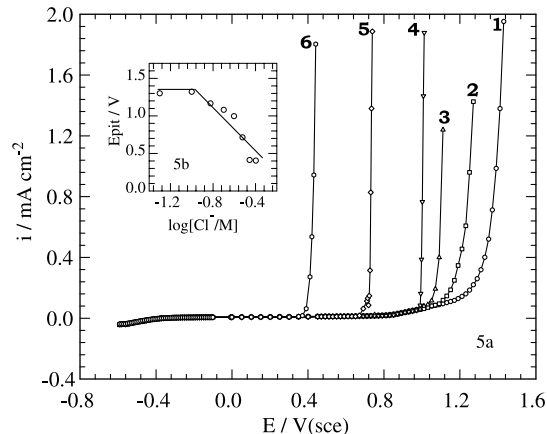


Fig. 5. (a) Effect of $[\text{Cl}^-]$ on the potentiodynamic polarization curves for type 304 SS in 0.25 M Na_2SO_4 at pH 10; (1) 0, (2) 0.15, (3) 0.20, (4) 0.25, (5) 0.35, (6) 0.50 M NaCl. (b) Variation of E_{pit} with $\log [\text{Cl}^-]$ for 304 SS in 0.25 M $\text{Na}_2\text{SO}_4 + x$ M NaCl at pH 10.

transpassivity was recorded. Addition of Cl^- shifted the polarization curves in the active direction and recorded current increased due to pitting corrosion.

The pitting potential, E_{pit} , was determined from the polarization curves at the point where a stable increase in current density takes place. Figure 5b shows the relationship between E_{pit} and the logarithm of $[\text{Cl}^-]$. The linear dependence of E_{pit} on $\log [\text{Cl}^-]$ can be represented as

$$E = A - B \log[\text{Cl}^-] \quad (7)$$

where A and B are constants depending on the nature of the electrode and the environment. The slope B of the linear part in Figure 5b equals 250 mV per decade. This value is higher than those calculated previously for the steel electrode in acidic and neutral solutions [5, 6].

The results in Figure 5b reveal that, when the $[\text{Cl}^-] \leq 0.15$ M, pitting occurs only in the transpassive region, or no pitting occurs at all, which suggests that at such low concentration, the Cl^- ions are unable to displace the adsorbed oxygen from the protective layer. However, at $[\text{Cl}^-] \geq 0.15$ M, pitting occurs in the passive region resulting in a shift of the polarization curves in the active direction (cf. Figure 5).

3.2.2. Effect of sulphate concentration

The effect of sulphate ion concentration on the pitting susceptibility of the steel electrode was also investigated. Figure 6a shows the potentiodynamic anodic polarization curves recorded for the steel electrode in 0.25 M NaCl solution containing different SO_4^{2-} concentrations in the range 0–0.5 M. It is clear that addition of SO_4^{2-} results in a shift of the polarization curves in the more noble direction. This indicates that the pitting resistance of the steel electrode increases by the addition of SO_4^{2-} . The variation of E_{pit} with sulphate ion concentration is shown in Figure 6b. Similar results were obtained previously upon the addition of HCO_3^- [9], SO_4^{2-} [5]

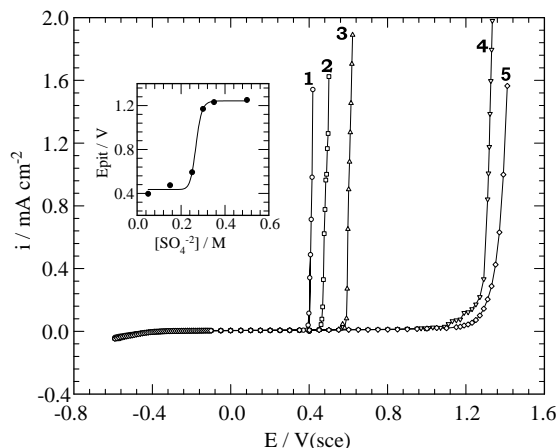


Fig. 6. (a) Effect of $[\text{SO}_4^{2-}]$ on potentiodynamic polarization curves for type 304 SS in 0.25 M NaCl + x M Na_2SO_4 at pH 10; (1) 0, (2) 0.05, (3) 0.15, (4) 0.25, (5) 0.35 M (b) Variation of E_{pit} with $\log [\text{SO}_4^{2-}]$ for 304 SS in 0.25 M NaCl + x M Na_2SO_4 of pH 10.

and OH^- [28] to solutions of constant chloride concentration.

At $[\text{SO}_4^{2-}] \geq 0.25$ M, a remarkable positive shift of the polarization curve was obtained (cf. Figure 6a) the observed current being characteristic of a transpassive reaction. Thus at $[\text{SO}_4^{2-}] \geq 0.25$ M, no pitting occurs. This behaviour may be attributed to the fact that the SO_4^{2-} adsorbate are less mobile and have higher adsorption strength than the Cl^- , especially in alkaline media [17]. The efficiency of Cl^- as a pitting agent is therefore markedly reduced in the presence of sulphate ions. The results show that sulphate ions have an inhibiting action on pitting corrosion of 304 stainless steel in chloride solution.

3.3. Potentiostatic polarization results

Passive films were formed on the steel electrode at different constant potentials in the range from -0.4 to 1.3 V. At each potential, the current transient was recorded for a period of 30 min, where steady state was reached. Impedance spectra were then recorded in the frequency range 0.1 to 10^5 Hz. The data are presented in Figure 7. At all potentials, there is a monotonic decrease in current with time until steady state is reached. At higher potentials, higher steady state currents were recorded. This may be attributed to the destabilization of the oxide film and the possibility of transpassive reaction. The initial rapid decrease in current density, i , with time is caused by fast formation and growth of the anodic passive film on the steel surface.

Figure 7a shows linear plot of the current density with time in a log scale for the steel electrode passivated at 0.3 V, as a typical example. Similar plots were also obtained at other passivation potentials. The relation between current and time can be represented as

$$i = at^{-n} \quad (8)$$

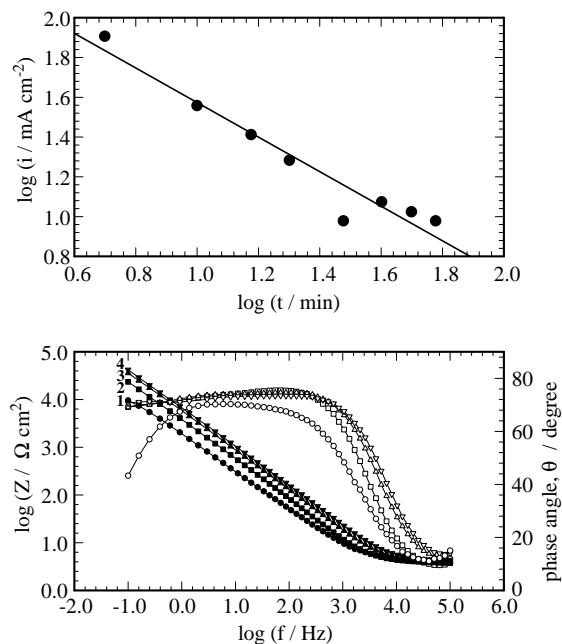


Fig. 7. (a) $\log i - \log t$ plot for type 304 SS passivated at 0.3 V in 0.25 M Na_2SO_4 of pH 10. (b) Bode plots of type 304 SS passivated at different potentials; (1) -0.40 , (2) -0.20 , (3) 0 and (4) 0.30 V.

where i is the anodic current density consumed in the oxide film formation. a is constant, t is the time and n represents a repassivation rate parameter. The value of n can be obtained from the slope of the linear region of the current transient in the logarithmic scale (Figure 7a). It may be considered as an indirect measure of the rate of oxide film formation. The calculated values of n is 0.8 , which shows a weak dependence on potential in the range of our investigation and the passivation process is under mixed control [11].

Figure 7b presents Bode plots recorded for the steel electrode passivated in 0.25 M Na_2SO_4 , solution of pH 10 at different constant potentials in the range -0.4 to 0.2 V. Other impedance spectra were also recorded at higher potentials (up to $E \leq 1.3$ V). The impedance spectra were analyzed as described in Section 3.1 for the open-circuit measurements using the equivalent circuit model of Figure 2b. The results of the fitting and the impedance data analyses are presented in Table 3. It is clear that R_p increases with passivation potential passing through a maximum at $E = 0.3$ V and then decreases rapidly with increasing passivation potential. The reverse trend was observed for the capacitance C indicating film thickening. At higher potentials there is a possibility of film breakdown leading to a decrease in R_p and an increase in C . The observed maximum at 0.3 V (Table 3) is attributed to the high stability of oxide films formed on steel in alkaline solutions at potentials ≤ 0.3 V [13].

A comparison between the behaviour of the passivated steel electrode in chloride-free and chloride containing sulphate solutions at pH 10 was made. This

Table 3. Equivalent circuit parameters for type 304 stainless steel passivated at different constant potentials in 0.25 M Na₂SO₄ of pH 10

E/V	$R_{\Omega}/\Omega \text{ cm}^2$	$R_p/M\Omega \text{ cm}^2$	$C/\mu\text{F cm}^{-2}$	α
-0.4	31.8	0.15	19.25	0.79
-0.2	30.2	1.95	15.73	0.84
0	32.0	2.77	9.18	0.83
0.2	33.6	3.24	6.76	0.82
0.3	32.4	4.38	6.70	0.85
0.4	32.0	1.97	9.18	0.80
0.6	32.1	1.14	12.14	0.83
0.7	32.1	0.66	20.73	0.80
0.8	32.2	0.30	24.85	0.80

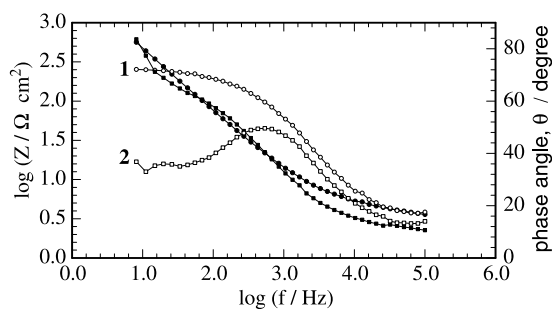


Fig. 8. Bode plots of type 304 SS passivated at 0.575 V in 0.25 M Na₂SO₄ of pH 10 at different [Cl⁻]; (1) 0 M NaCl and (2) 0.25 M NaCl.

comparison is presented in the Bode plot format of Figure 8. This figure shows that, in pure Na₂SO₄ solution, the impedance spectrum is highly capacitive with one time constant and the electrode surface is characterized by a high impedance value, which indicates that the electrode is passive. In the presence of chloride the impedance of the electrode is decreased and the phase angle shows a splitting corresponding to more than one time constant.

4. Conclusions

- Type 304 stainless steel passivates in alkaline sulphate solutions under open-circuit conditions, and the passivation process follows a simple logarithmic law.
- Pitting corrosion of the steel occurs at [Cl⁻] ≥ 0.15 M, the sulphate ion acts as a pitting inhibitor and at [SO₄²⁻] ≥ 0.25 M no pitting was recorded.
- The electrode/electrolyte interface can be described by an equivalent circuit model consisting of a par-

allel combination of a constant phase element, Q , and a passive film resistance, R_p , both in series with the solution resistance, R_{Ω} .

References

1. C.R. Clayton and I. Olefjord; in Corrosion Mechanisms in Theory and Practice, P. Marcus and J. Oudar, Editors, p 175, Marcel Dekker, New York (1995), and references therein.
2. E. De Vito and P. Marcus, Surf. Interf. Anal, **19** (1992) 403.
3. W. Wang, D. Costa and P. Marcus, J. Electrochem. Soc., **141** (1994) 111.
4. V. Maricue, W. Yang and P. Marcus, J. Electrochem. Soc., **143** (1996) 1182.
5. S.S. El-Egamy, W.A. Badawy and H. Shehata, Corrosion Prevention Control, **47** (2000) 35.
6. S.S. El-Egamy, W.A. Badawy and H. Shehata, Mat. Wiss. und Werkstofftech, **31** (2001)737.
7. S.I. Ali and G.J. Abbaschian, Corros. Sci., **18** (1978)15.
8. H.C. Man, D.R. Gabe, Corros. Sci., **21** (1981) 713.
9. J.J. Park, S.I. Pyun, W.J. Lee and H.P. Kim, Corrosion, **55** (1999) 380.
10. A.R. Brooks, C.R. Clayton, K. Doss and Y.C. Lu, J. Electrochem. Soc., **133** (1986) 2459.
11. T. Hong, G.W. Walter and M. Nagumo, Corros. Sci., **38** (1996) 1525.
12. J.H. Wang, C.C. Su and Z. Zsklarska-Smialowska, Corrosion, **44** (1988) 732.
13. S.T. Amaral and I.L. Muller, Corros. Sci., **41** (1999) 747.
14. T. Kodoma, 5th Int. Congr. Metallic Corrosion, p. 223, NACE, Houston 1974.
15. R.P. Frankenthal and H.W. Pickering, J. Electrochem. Soc., **119** (1972) 1304.
16. Z. Szklarska-Smialowska, Corros. Sci., **18** (1978) 97.
17. A. Kolics, J.C. Polkinghorne and A. Wieckowski, Electrochim. Acta, **43** (1998) 2605.
18. M. Keddum, O. R. Mattos and H. Taken; Electrochim. Acta, **31** (1986) 1159.
19. A. L. Dobbelaar, E. C. M. Herman and J. H. W. De Wit; Corros. Sci., **33** (1992) 765.
20. D. D. Macdonald and Urquidi-Macdonald in Modification of Passive Films; P. Marcus, B. Baroux and M. Keddum, Editors, p. 46, Ins. Of Materials, London (1994).
21. D. D. Macdonald, S. R. Biaggio and H. Song; J. Electrochem. Soc., **139** (1992) 17.
22. J.R. Macdonald, "Impedance Spectroscopy" New York, N.Y., John Wiley & Sons, 1987.
23. K. Juttner, W.J. Lorenz and W. Paatsch, Corros. Sci., **29** (1989) 279.
24. U. Rammelt and R. Reinhard, Corros. Sci., **27** (1987) 373.
25. K. Juetner, W.J. Lorenz, W. Paatsch, M.W. Kendig and F. Mansfeld, Werkst. und Korros., **36** (1985) 120.
26. S.C. Thomas and V.I. Birss, J. Electrochem. Soc., **144** (1997) 1353.
27. J.W. Diggle, T.C. Downie and C.W. Goulding, Electrochim. Acta, **15** (1970) 1079.
28. S.M. Abd El-Motaal, N.H. Hilal and W.A. Badawy, Electrochim. Acta, **39** (1994) 3611.